EFFECTS OF MODES OF INITIAL IMPERFECTIONS ON THE STABILITY OF CYLINDRICAL SHELLS UNDER AXIAL COMPRESSION

By L. H. N. Lee

University of Notre Dame

SUMMARY

The effects of definite and "indefinite" initial imperfections on the buckling and postbuckling behavior of an axially compressed cylindrical shell are analyzed by a non-linear theory. The definite initial imperfections considered do not contribute to the reduction of the peak buckling load; while the "indefinite" imperfections, expressed in terms of a single factor introduced by Donnell[1], cause a reduction in the buckling strength. The physical meaning of the imperfection factor, however, needs further clarification. Two theoretical buckling processes are found to be possible. In the early stage of buckling, the cylinder may deform with a comparatively large number of waves of small amplitudes or the cylinder may deform with a comparatively small number of waves of large amplitudes. Further theoretical and experimental studies of the effects of initial imperfections and the process of buckling are suggested.

INTRODUCTION

The problem of elastic buckling of axially compressed cylindrical shells has not yet been completely solved in spite of being the subject of intensive research in recent years. To explain the fact that buckling loads obtained by experiments are much lower than that predicted by the classical linear theory[2,3], Donnell (1934) introduced a non-linear theory and the concept of initial imperfections. The non-linear theory was further developed by von Kármán and Tsien (1941)[4]. Their analysis, in turn, was refined by Leggett and Jones (1942)[5], Michielsen (1948)[6], and Kempner (1954)[7].

The non-linear theory does indicate a large drop of resistance as soon as buckling takes place. This is consistent with the observed phenomena. For a conceptually perfect cylinder, however, the buckling load predicted by the non-linear theory is still the same as that given by the classical theory. By considering the effects of initial imperfections, Donnell and Wan [8] were able to explain in a reasonable way the discrepancies between experimental and theoretical buckling loads. For the convenience of analysis, Donnell assumes that the geometrical and material imperfections of a cylinder may be replaced by an equivalent geometrical deviation. He assumes further that the equivalent geometrical deviation is proportional to the deformation of the cylinder and may be expressed by a single imperfection factor indicating essentially its magnitude. It is the purpose of this paper to evaluate the implication of this assumption.

Timoshenko[9] has shown, by a linear theory, that the initial curvature of an axially compressed, elastic column has substantial effects on the load-deflection relationship but relatively little effect on the maximum load. The initial shape of the column can be expressed by a series of functions giving the normal buckling mode shapes of the column. According to the linear theory, the term in the series describing the principal buckling mode has the predominant effect on the behavior of the column. In general, an axially compressed column having arbitrary small initial deviation most likely buckles in its principal mode. The assumption made by Donnell and Wan is apparently in accord with this fact. However, it has been shown[10] that the mode as well as the amplitude of the initial imperfections of a geometrically or physically non-linear structure may influence the buckling load and the corresponding mode of buckling. Therefore, the effects of definite initial imperfections as well as "indefinite" initial imperfections, in terms of the imperfection factor introduced by Donnell, on the buckling behavior of axially compressed cylinders are analyzed in this paper.

The present analysis is based on the Love-Kirchoff assumption for thin shells and the principle of stationary potential energy for load-deformation relationships.

ANALYSIS

Strain-Displacement Relationships

Consider an initially imperfect but nearly circular cylindrical shell of mean radius r, length L, and thickness t. Let the radial difference between the radial distance of a point at the initial median surface and the mean radius be denoted by w_o. Let x, s and z (positive inward) be the axial, circumferential and radial coordinate, respectively. The corresponding components of the displacement of the point, denoted by u, v and w (positive inward) respectively, are measured from the position at the initial median surface. Based on Donnell's assumptions[8], it may be shown that the bending strains depend only on the axial and circumferential curvature changes, $(\partial^2 w/\partial x^2)$ and $(\partial^2 w/\partial s^2)$, and the twist of the median surface $(\partial^2 w/\partial x \partial s)$. Including the effects of the initial radial deviations and the second order terms, the axial and circumferential membrane strains, ε_x and ε_s, and the membrane shear strain γ_{xs}, are[11]

$$
\begin{aligned}
\varepsilon_x &= \frac{\partial u}{\partial x} + \frac{1}{2}\left(\frac{\partial w}{\partial x}\right)^2 + \frac{\partial w}{\partial x}\frac{\partial w_o}{\partial x} \\
\varepsilon_s &= \frac{\partial v}{\partial s} + \frac{1}{2}\left(\frac{\partial w}{\partial s}\right)^2 + \frac{\partial w}{\partial s}\frac{\partial w_o}{\partial s} - \frac{w}{r} \qquad (1) \\
\gamma_{xs} &= \frac{\partial u}{\partial s} + \frac{\partial v}{\partial x} + \frac{\partial w}{\partial x}\frac{\partial w}{\partial s} + \frac{\partial w}{\partial x}\frac{\partial w_o}{\partial s} + \frac{\partial w_o}{\partial x}\frac{\partial w}{\partial s}
\end{aligned}
$$

The axial, circumferential and shear membrane stress, σ_x, σ_s and τ_{xs}, may now be expressed in terms of the membrane strains, the modulus of elasticity E and the Poisson's ratio ν by the Hooke's law for the isotropic material.

Equilibrium and Compatibility Equations

By omitting higher-order terms, it may be shown that the membrane stresses satisfy the equilibrium equations

$$\frac{\partial \sigma_x}{\partial x} + \frac{\partial \tau_{xs}}{\partial s} = 0$$
$$\frac{\partial \tau_{xs}}{\partial x} + \frac{\partial \sigma_s}{\partial s} = 0 \qquad (2)$$

Equations (2) are identically satisfied by the introduction of the Airy stress function $\phi(x,y)$ defined by the relations

$$\sigma_x = \frac{\partial^2 \phi}{\partial s^2}, \quad \sigma_s = \frac{\partial^2 \phi}{\partial x^2}, \quad \tau_{xs} = -\frac{\partial^2 \phi}{\partial x \partial s} \qquad (3)$$

By Hooke's law, the membrane strains may be expressed as

$$\epsilon_x = \frac{1}{E}\left(\frac{\partial^2 \phi}{\partial s^2} - \nu \frac{\partial^2 \phi}{\partial x^2}\right)$$
$$\epsilon_s = \frac{1}{E}\left(\frac{\partial^2 \phi}{\partial x^2} - \nu \frac{\partial^2 \phi}{\partial s^2}\right) \qquad (4)$$
$$\gamma_{xs} = -\frac{2(1+\nu)}{E} \frac{\partial^2 \phi}{\partial x \partial s}$$

Elimination of axial and circumferential displacement components between Eqs. (1) and combination of Eqs. (1) and (4) yield the compatibility equation

$$\nabla^4 \phi = E\left[\left(\frac{\partial^2 w}{\partial x \partial s}\right)^2 - \frac{\partial^2 w}{\partial x^2}\frac{\partial^2 w}{\partial s^2} - \frac{1}{r}\frac{\partial^2 w}{\partial x^2} + 2\frac{\partial^2 w}{\partial x \partial s}\frac{\partial^2 w_o}{\partial x \partial s} - \frac{\partial^2 w}{\partial x^2}\frac{\partial^2 w_o}{\partial s^2} - \frac{\partial^2 w_o}{\partial x^2}\frac{\partial^2 w}{\partial s^2}\right] \qquad (5)$$

in which $\nabla^4 = \left(\frac{\partial^4}{\partial x^4} + 2\frac{\partial^4}{\partial x^2 \partial s^2} + \frac{\partial^4}{\partial s^4}\right)$

The stress function and the membrane stresses may now be determined by Eq. (5) if the initial imperfection and the the radial displacement are obtained or assumed.

Initial Imperfections and Deformations

The initial geometrical imperfections or the deformation of the cylinder can be completely described by an infinite double Fourier series. The degree of approximation which can be attained in the description largely depends on the choice of a proper number of terms of the series. However, the mathematical difficulties of solving the problem multiply rapidly with increasing number of terms considered. To simplify the analysis, it is assumed that the initial radial deviation may be described by

$$w_o = At \cos \frac{\pi x}{L_x} \cos \frac{\pi s}{L_s} + \frac{a_o}{a} w \qquad (6)$$

where A and a_o are the given or known dimensionless amplitude parameters, L_x and L_s are the given or known half wave lengths in the axial and circumferential directions respectively. The first term at the right-hand side of Eq. (6) describes a definite shape. The second term, introduced by Donnell [8], is definite in amplitude but indefinite in shape, because the radial displacement w varies with the applied load. It may be interpreted that the second term is used to replace all terms in the infinite series which may have effects on the deformation. It also implies that only one of these implicit terms influences the deformation at one time.

The deformation of the cylinder is assumed to be given by

$$w = at \left[\cos \frac{\pi x}{\ell_x} \cos \frac{\pi s}{\ell_s} + b \cos \frac{2\pi x}{\ell_x} + d \right] \qquad (7)$$

where a and b are arbitrary parameters, ℓ_x and ℓ_s are the unknown half-wave lengths of the deformation waves in the axial and circumferential directions. d is not an independent parameter. d may be determined by the condition that v is a periodic function of s. The deformation function by Eq. (7) is essentially the one adopted by Donnell [8] and Kempner [7] except that a term of $\cos \frac{2\pi s}{\ell_s}$ is not included.

Stress Function

By introducing w_o from Eq. (6) and w from Eq. (7) into Eq. (5), the stress function is found to be

$$
\begin{aligned}
\phi = -\frac{Et^2}{\mu^2\eta}\Bigg\{ & \frac{a(aK\eta - 8b)}{32}\cos\frac{2\pi x}{\ell_x} + \frac{a^2K\eta\mu^4}{32}\cos\frac{2\pi s}{\ell_s} + \\
& a(2abK\eta-1)P_{11}^{2}\cos\frac{\pi x}{\ell_x}\cos\frac{\pi s}{\ell_s} + 2a^2bK\eta\, P_{31}^{2}\cos\frac{3\pi x}{\ell_x}\cos\frac{\pi s}{\ell_s} \\
& + \frac{Aa\eta_o}{4}\Bigg[\frac{\mu^2}{(\mu-\mu_o)^2}\bigg[Q_{11}^{2}\cos\frac{(\mu n-\mu_o n_o)x}{r}\cos\frac{(n-n_o)s}{r} \\
& + Q_{22}^{2}\cos\frac{(\mu n+\mu_o n_o)x}{r}\cos\frac{(n+n_o)s}{r}\bigg] + \frac{\mu^2}{(\mu+\mu_o)^2}\cdot\bigg[\\
& Q_{12}^{2}\cos\frac{(\mu n-\mu_o n_o)x}{r}\cos\frac{(n+n_o)s}{r} + Q_{21}^{2}\cos\frac{(\mu n+\mu_o n_o)x}{r}\cdot \\
& \cos\frac{(n-n_o)s}{r}\bigg] + 8b\bigg[Q_{33}^{2}\cos\frac{(2\mu n-\mu_o n_o)x}{r}\cos\frac{n_o s}{r} \\
& + Q_{44}^{2}\cos\frac{(2\mu n+\mu_o n_o)x}{r}\cos\frac{n_o s}{r}\bigg]\Bigg]\Bigg\} - \frac{\sigma s^2}{2}
\end{aligned} \qquad (8)
$$

in which

$$K = 1 + \frac{2a_o}{a} = 1 + \frac{V}{a}, \quad \mu = \frac{\ell_s}{\ell_x}, \quad \mu_o = \frac{L_s}{L_x}$$

$$n = \frac{\pi r}{\ell_s}, \quad n_o = \frac{\pi r}{L_s}, \quad \eta = \frac{n^2 t}{r}, \quad \eta_o = \frac{n_o^{2} t}{r}$$

$$P_{11} = \frac{\mu^2}{1+\mu^2}\ , \quad P_{31} = \frac{\mu^2}{1+9\mu^2}\ , \quad \alpha = \sqrt{\frac{\eta_o}{\eta}}$$

$$Q_{11} = \frac{(\mu-\mu_o)^2}{(\mu-\alpha\mu_o)^2+(1-\alpha)^2}\ , \quad Q_{22} = \frac{(\mu-\mu_o)^2}{(\mu+\alpha\mu_o)^2+(1+\alpha)^2}$$

$$Q_{12} = \frac{(\mu+\mu_o)^2}{(\mu-\alpha\mu_o)^2+(1+\alpha)^2}\ , \quad Q_{21} = \frac{(\mu+\mu_o)^2}{(\mu+\alpha\mu_o)^2+(1-\alpha)^2}$$

$$Q_{33} = \frac{\mu^2}{(2\mu-\alpha\mu_o)^2+\alpha^2}\ , \quad Q_{44} = \frac{\mu^2}{(2\mu+\alpha\mu_o)^2+\alpha^2}$$

In Eq. (8) σ is the applied average axial compressive stress.

Potential Energy

The total potential energy of the system consists of the potential energy of the applied load and the internal strain energy in the cylinder. There are two parts in the strain energy, the membrane strain energy U_m and the bending strain energy U_b. They can be expressed as

$$U_m = \frac{t}{2E}\int_0^L\int_0^{2\pi r}\left[(\sigma_x+\sigma_s)^2 - 2(1+\nu)(\sigma_x\sigma_s - \tau_{xs}^2)\right]dxds \tag{9}$$

and

$$U_b = \frac{D}{2}\int_0^L\int_0^{2\pi r}\left\{(\nabla^2 w)^2 + 2(1-\nu)\left[\left(\frac{\partial^2 w}{\partial x\partial s}\right)^2 - \frac{\partial^2 w}{\partial x^2}\frac{\partial^2 w}{\partial s^2}\right]\right\}dxds \tag{10}$$

in which $D = (1/12)\,Et^3/(1-\nu^2)$.

From Eqs. (3), (4), (7), (8), (9) and (10), the total internal strain energy, U_i , is found to be

$$
\begin{aligned}
U_i = (\pi E t^3 L/r) \Big\{ & a^2(aK\eta - 8b)^2/128 + a^4K^2\eta^2\mu^4/128 \\
& + a^2(2abK\eta-1)^2 P_{11}^{\;2}/4 + a^4b^2K^2\eta^2 P_{31}^{\;2} \\
& + (A^2a^2\eta_o^2/64)\Big[Q_{11}^{\;2} + Q_{22}^{\;2} + Q_{12}^{\;2} + Q_{21}^{\;2} \\
& + 64b^2(Q_{33}^{\;2} + Q_{44}^{\;2})\Big] + (\sigma r/Et)^2 \\
& + \left[a^2\eta^2/48\cdot(1-\nu^2)\right]\left[(1 + \mu^2)^2 + 32b^2\mu^4\right]\Big\}
\end{aligned} \tag{11}
$$

The potential energy of the axial load applied to the ends of the cylinder, U_a, can be expressed as

$$U_a = 2\pi r t\,\sigma \int_0^L \left(\frac{\partial u}{\partial x}\right) dx \tag{12}$$

The integral in Eq. (12) gives the total end shortening in the axial direction. From the first of Eqs. (1) and the first of Eq. (4), the integrand is found to be

$$\frac{\partial u}{\partial x} = \frac{1}{E}\left(\frac{\partial^2\phi}{\partial s^2} - \nu\,\frac{\partial^2\phi}{\partial x^2}\right) - \frac{1}{2}\left(\frac{\partial w}{\partial x}\right)^2 - \left(\frac{\partial w}{\partial x}\right)\left(\frac{\partial w_o}{\partial x}\right) \tag{13}$$

If ε is defined as the average unit end shortening in the axial direction or the ratio of the total end shortening and the cylinder length, it is found that

$$(\varepsilon r/t) = (\sigma r/Et) + a^2K\eta\mu^2\,(1 + 8b^2)/8 \tag{14}$$

In carrying out the integral in Eq. (12), it is assumed that $\ell_x \neq L_x$ and that the initial and deformed axial wave lengths are small compared to the entire length of the cylinder.

Determination of Parameters

The deflection parameters, expressed in terms of a, b, η and μ, may be determined by the principle of stationary potential energy. When the total potential energy of the system, $U_1 + U_a$, is made stationary for a small variation of each of the four parameters, the following four simultaneous algebraic equations are obtained:

$$(aK\eta - 8b)\left[a\eta(1+K) - 8b\right] + a^2K\eta^2\mu^4(1 + K) + 32 \cdot$$

$$(2abK\eta - 1)\left[2ab\eta(1 + K) - 1\right] P_{11}^2 + 128\ a^2b^2\eta^2K \cdot$$

$$(1 + K)P_{31}^2 + 2A^2\eta_o^2 \left[Q_{11}^2 + Q_{22}^2 + Q_{12}^2 + Q_{21}^2 + \right.$$

$$\left. 64b^2(Q_{33}^2 + Q_{44}^2)\right] + 8\eta^2\left[(1 + \mu^2)^2 + 32b^2\mu^4\right]/3(1-\nu^2)$$

$$- 16(\sigma r/Et)\eta\mu^2(1 + K)(1 + 8b^2) = 0 \qquad (15)$$

$$b = aK\eta\left[(1/8) + P_{11}^2\right] \div \left[1 + 2a^2K^2\eta^2(P_{11}^2 + P_{31}^2)\right.$$

$$+ 2A^2\eta_o^2\ (Q_{33}^2 + Q_{44}^2) + 4\eta^2\mu^4/3(1-\nu^2)$$

$$\left. - 4(\sigma r/Et)\eta K\mu^2\right] \qquad (16)$$

$$a^2K^2\eta\ (1 + \mu^4) - 8abK + 64abK(2abK\eta - 1)P_{11}^2$$

$$+ 128\ a^2b^2K^2\eta\ P_{31}^2 + 2A^2\eta_o\alpha^3 \left\{Q_{22}^3\left[\mu_o(\mu + \alpha\mu_o)\right.\right.$$

$$+ 1 + \alpha\Big] / (\mu-\mu_o)^2 - Q_{11}^{\,3}\Big[\mu_o(\mu-\alpha\mu_o) + 1-\alpha\Big] /(\mu-\mu_o)^2$$

$$+ Q_{21}^{\,3}\Big[\mu_o(\mu+\alpha\mu_o) - 1 + \alpha\Big] /(\mu + \mu_o)^2$$

$$- Q_{12}^{\,3}\Big[\mu_o(\mu - \alpha\mu_o) - 1 - \alpha\Big] /(\mu + \mu_o)^2$$

$$+ (128\ A^2b^2\eta_o\ \alpha^3/\mu^2)\Big\{\Big[\mu_o(2\mu + \alpha\mu_o) + \alpha\Big] Q_{44}^{\,3}$$

$$- \Big[\mu_o(2\mu - \alpha\mu_o) - \alpha\Big] Q_{33}^{\,3} \Big\}$$

$$+ 8\eta \Big[(1 + \mu^2)^2 + 32\ b^2\mu^4\Big]/3(1 - \nu^2)$$

$$- 16\ (\sigma r/Et)\ K\mu^2\ (1 + 8b^2) = 0 \qquad (17)$$

$$a^2K^2\eta^2\mu^3/32 + (2abK\eta - 1)^2P_{11}^{\,3}/\mu^3$$

$$+ 4a^2b^2K^2\eta^2\ P_{31}^{\,3}/\mu^3 + (A^2\eta_o^{\,2}/16)\Big\{$$

$$(1 - \alpha)\Big[\mu_o(\mu - \alpha\mu_o) + 1 - \alpha\Big] Q_{11}^{\,3}/(\mu - \mu_o)^3$$

$$+ (1 + \alpha)\Big[\mu_o(\mu + \alpha\mu_o) + 1 + \alpha\Big]Q_{22}^{\,3}/(\mu - \mu_o)^3$$

$$+ (1 + \alpha)\Big[1 + \alpha - \mu_o(\mu - \alpha\mu_o)\Big]Q_{12}^{\,3}/(\mu + \mu_o)^3$$

$$+ (1 - \alpha)\Big[1 - \alpha - \mu_o(\mu + \alpha\mu_o)\Big]Q_{21}^{\,3}/(\mu + \mu_o)^3\Big\}$$

$$+ (4\alpha A^2b^2\eta_o^{\,2}/\mu^3)\Big\{\Big[\alpha - \mu_o(2\mu - \alpha\mu_o)\Big]Q_{33}^{\,3}$$

$$+ \Big[\alpha + \mu_o(2\mu + \alpha\mu_o)\Big]\ Q_{44}^{\,3}\Big\}$$

$$+ \eta^2\mu\left[1 + \mu^2 + 32b^2\mu^2\right]/12(1 - \nu^2)$$

$$- (\sigma r/Et)\, K\eta\mu(1 + 8b^2)/2 = 0 \tag{18}$$

In the variational procedure, it is considered that σ = constant, the case of dead-weight loading. The deflection parameters for a given load may now be determined by solving Eqs. (15) to (18) simultaneously. The following procedure of obtaining numerical solutions is considered.

Eq. (16) is first used to eliminate b from the other three equations. The values of the parameters, A, a_o, η_o and μ_o defining the initial imperfections are preassigned. For assumed values of a, η, and μ, a value of σ may be computed from each of the three equations. The correct set of a, μ, and η yields the same σ value from each of the three equations. For a fixed value of a, a pair of η and μ may be found by systematic coarse scanning such that the three corresponding values of σ are reasonably close to each other. Then by keeping one of the two parameters constant and adding a small increment to the other one, the effects of the increment on the σ-values are determined. Knowing these effects, a new pair of η and μ may be extrapolated. This process may be repeated until a pair of η and μ values are found such that the three σ-values agree with each other to within a desired accuracy.

For a fixed value of a, there may be more than one set of η, μ and σ values satisfying the three equations. Knowing a set of a, η, μ and σ values, the corresponding values of b and $(\epsilon r/t)$ may be calculated by Eqs. (16) and (14). The entire procedure may be repeated for a suitable number of a-values. The computation involved in this method of solution was programmed by the Fortran language on an IBM 1620 digital computer.

NUMERICAL RESULTS AND DISCUSSIONS

The numerical results of the solution of Eqs. (15) to (18) for a number of cases are shown in Figs. 1 to 6 as functions of the unit end shortening parameter $(\epsilon r/t)$. For comparison, the $(\sigma r/Et)$ vs $(\epsilon r/t)$ relationship of a perfect cylinder, Case I: $A = 0$, $V = 0$, is also shown in Fig. 1. For this case, the minimum value of the applied stress in the postbuckling region is $\sigma = 0.193\ (Et/r)$ at $\mu = 0.397$ and $(\epsilon r/t) = 0.462$. These results compare favorably with the corresponding results of $\sigma = 0.195\ (Et/r)$ at $\mu \cong 0.40$ by Leggett and Jones[5] and Michielsen[6]. The minimum stress obtained by Kempner[7], by using five parameters in the variational procedure, is $0.182\ (Et/r)$ at $\mu = 0.362$. Fig. 1 shows the departure of the results by the present analysis and that of Michielsen[6] in the region $(\epsilon r/t) > 0.5$. The difference is due to the deformation functions employed in the two analyses being slightly different. The results of the present analysis in the region $(\epsilon r/t) > 0.5$ practically coincide with that by Kempner[7]. The variations of the deflection parameters with unit shortening for this case are shown in Fig. 2.

Fig. 1 also shows the $(\sigma r/Et)$ vs $(\epsilon r/t)$ curves of three other cases having essentially definite initial imperfections. These curves deviate only slightly from that of the perfect cylinder. It is also to be noted that the values of the parameters defining the initial imperfections are in the critical ranges of the deflection parameters giving the shapes of the deformation waves of the perfect cylinder. The maximum applied stress for Case II is $0.621\ (Et/r)$. For cases III and IV it is $0.617\ (Et/r)$. These maximum stresses are slightly higher than the critical value of $0.605\ (Et/r)$ for the perfect cylinder. It indicates that definite initial imperfections, at least, of the type considered do not cause lower buckling stresses. However, the characteristics of the curves in Fig. 1 indicate that the imperfect cylinders, when subject to external disturbances, may become unstable at critical stresses less than the maximum applied stresses and snap through into other states of equilibrium which are connected with considerably smaller axial loads. But, it is to be noted that the imperfect cylinders II, III and IV are comparatively more stable than the perfect cylinder. The curves indicate that a comparatively larger amount of external disturbance may be needed to cause the snapthrough bucklings of the imperfect cylinders than that of the perfect cylinder.

Although the $(\sigma r/Et)$ vs $(\varepsilon r/t)$ curves of the imperfect and perfect cylinders appear to be similar, their deflection parameters do not vary in a similar manner. Fig. 3 shows the variations of the deflection parameters with unit end shortening for Case II, which are similar to that of Case I. However, the variations of the deflection parameters with unit end shortening for Case IV, shown in Fig. 4, (similar results for Case III) are quite different from the other two cases. It indicates that the initial imperfections may affect the buckling process of a cylinder. It also indicates that the following two buckling processes are possible. In the early stage of buckling, a cylinder may deform with a comparatively small number of waves of comparatively large amplitudes (Case II) or a cylinder may deform with a comparatively large number of waves of comparatively small amplitudes (Case IV).

Fig. 5 represents the influences of the imperfection factor, V, $(V = 2a_o)$, on the behavior of an axially compressed cylinder. The segment of Curve 1 in solid line was obtained by the process previously described. The minimum applied stress indicated by Curve I is 0.187 (Et/r) at $(\varepsilon r/t) = 0.451$ and $\mu = 0.349$. In the region of the dotted line of Curve 1, an exhaustive search did not produce a set of parameters that satisfies the three simultaneous equations. However, other sets of parameters that yield points in the $(\sigma r/Et)$ vs $(\varepsilon r/t)$ plane above Curve 1 were found. This difficulty may be due to the insufficient number of terms included in the deflection function.

Curve 2 in Fig. 5 was obtained by using the following deflection function previously employed by Loo[12].

$$w = a't\left[\sin\frac{ns}{r}\sin\frac{\pi x}{\ell_x} + b'\left(\cos\frac{2\pi x}{\ell_x} - 1\right) + d'\right] \quad (19)$$

It may be shown that the total potential energy of a cylinder having the initial imperfection given by Eq. (6) and the deflection given by Eq. (19) may still be expressed by Eqs. (11), (12), and (14) provided that a is replaced by a' and b is replaced by $(-b')$ in these equations. By using a numerical procedure identical to the previous one, Curve 2 in Fig. 5 as well as the variations of the parameters with unit end shortening shown in Fig. 6 were obtained. For comparison, Fig. 5 also shows the results by Loo[12] for cases of $V = 0$ and $V = .2$. These results, which compared reasonably well with that of the present analysis, were obtained by assuming the constant values of η and μ given by the classical small deflection theory. It is to be noted that the values of a' in Fig.6 are much less than the values of a of the Cases I to IV. It is also to be noted that the values of η and μ in Fig. 6 are close to the corresponding values predicted by the small-deflection theory. The results also indicate that the number of waves, given by η, decreases in the later stage of the buckling process. This has also been indicated by Von Karman and Tsien[4].

CONCLUDING REMARKS

The foregoing analysis and numerical results indicate that the theoretical axial buckling stresses of cylinders having definite initial imperfections, at least of the periodic type considered, are not necessarily lower than that of a perfect cylinder. In other words, it is possible that certain types of definite initial deviations may increase the buckling resistance of a cylindrical shell. The imperfection factor introduced by Donnell[1] leads to lower theoretical buckling stresses. However, the physical meaning of the factor needs further clarification.

The usage of the imperfection factor implies the following assumption. The initial imperfections may be described by an infinite double Fourier series having all terms, each of which is a function of the space coordinates only, of equal amplitude; the terms interact with the deflection function, a function of the space coordinates and the applied load one at a time. However, the present analysis indicates that all the terms may interact with the deflection function. The interactions may not necessarily reduce the theoretical buckling stress.

It has also been found that two theoretical buckling processes are possible. In the early stage of buckling, a cylinder may deform with a comparatively large number of waves of comparatively small amplitudes or it may deform with a comparatively small number of waves of comparatively large amplitudes.

It is obvious that further research on the effects of initial imperfections and the process of buckling is needed. The theoretical analysis may be improved by considering (a) higher order terms in the strain-displacement relationships and the equilibrium equations, and (b) more accurate descriptions of the initial imperfections and the deflection. From the present analysis, it appears that aperiodic as well as periodic functions should be used to describe the initial imperfections and the deflection.

A great deal of mathematical difficulty is expected in any theoretical refinement. They may be alleviated, however, if the theoretical development is guided by refined experiments. Most of the experimental results available in the literature are usually presented in terms of only the critical buckling load and the final mode of buckling. New experimental results on the complete development of the buckling stress pattern, prebuckling and postbuckling, may provide a physical basis for a better theoretical insight into this difficult problem.

REFERENCES

1. Donnell, L. H.: A New Theory for the Buckling of Thin Cylinders under Axial Compression. Trans. ASME, Vol. 56, 1934, p. 795.

2. Timoshenko, S.: Einige Stabilitatsprobleme der Elastizitatstheorie. Z. Math. Phys., Vol. 58, No. 4, 1910, p. 337.

3. Southwell, R. V.: On the General Theory of Elastic Stability. Phil. Mag., Series A, Vol. 213, 1914, p. 187.

4. Von Kármán, Th., and Tsien, H. S.: The Buckling of Thin Cylindrical Shells under Axial Compression. J. Aeronaut. Sci., Vol. 8, No. 8, 1941, p. 303.

5. Leggett, D. M. A., and Jones, R. P. N.: The Behavior of a Cylindrical Shell under Axial Compression when the Buckling Load has been Exceeded. A.R.C.R. and M., No. 2190, Aug. 1942.

6. Michielsen, H. F.: The Behavior of Thin Cylindrical Shells After Buckling under Axial Compression. J. Aeronaut. Sci., Vol. 15, No. 12, 1948, p. 739.

7. Kempner, J.: Postbuckling Behavior of Axially Compressed Circular Cylindrical Shells. J. Aeronaut. Sci., Vol. 21, No. 5, 1954, p. 329.

8. Donnell, L. H. and Wan, C. C.: Effects of Imperfections on Buckling of Thin Cylinders and Colmns Under Axial Compression. Trans. ASME, Vol. 72, No. 1, 1950, p. 73.

9. Timoshenko, S. and Gere, J. M.: Theory of Elastic Stability. McGraw-Hill Book Co., New York, 1961, p. 31.

10. Lee, L. H. N.: Stability of Non-Linear Systems. J. Engr. Mech., ASCE Proceedings, Vol. 88, No. EM2, Part 1, April, 1962, p. 81.

11. Thielemann, W. F.: New Developments in the Non-linear Theories of the Buckling of Thin Cylindrical Shells. Aeronautics and Astronautics, Pergamon Press, New York, 1960, p. 76.

12. Loo, T. T.: Effects of Large Deflections and Imperfections on the Elastic Buckling of Cylinders under Torsion and Axial Compression. Proc. 2nd U. S. Congr. Appl. Mechanics, 1954, p. 345.

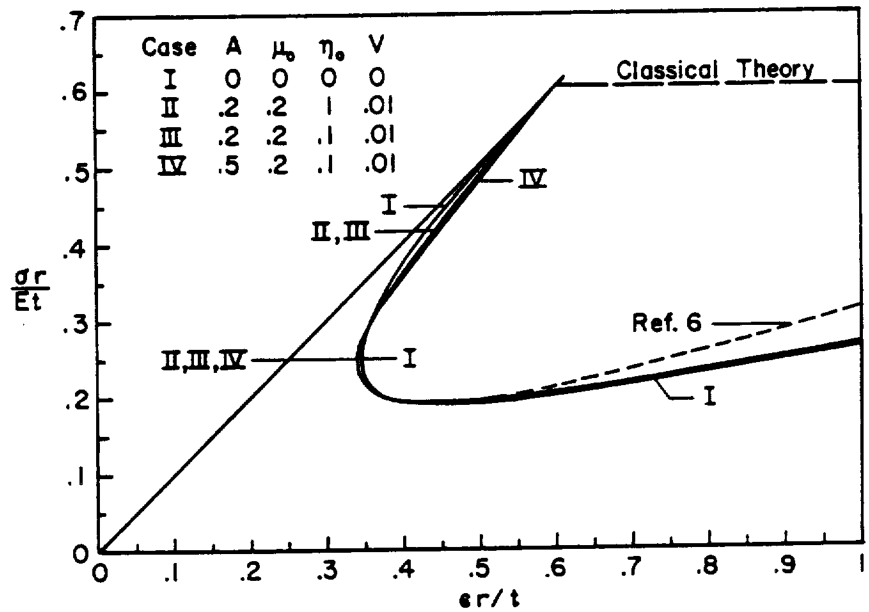

Figure 1.- Variation of applied stress with unit end shortening.

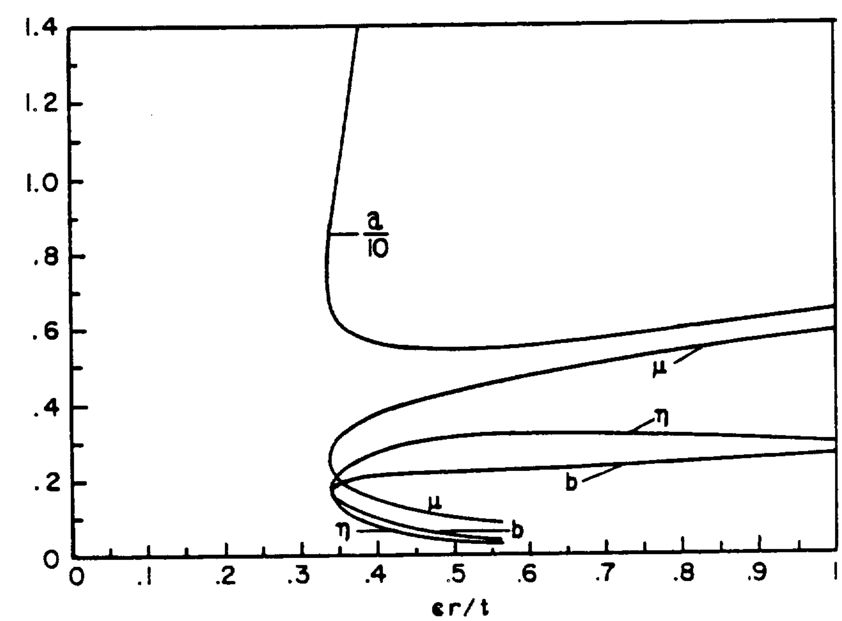

Figure 2.- Variation of deflection parameters with unit end shortening.
Case I: $A = 0$; $V = 0$.

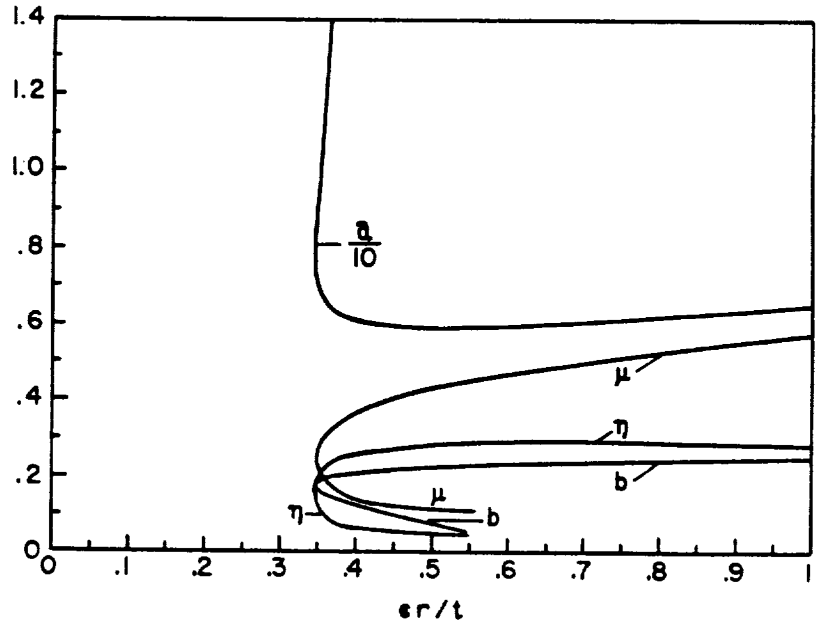

Figure 3.- Variation of deflection parameters with unit end shortening. Case II: $A = .2$; $\eta_o = 1.0$; $\mu_o = .2$; $V = .01$.

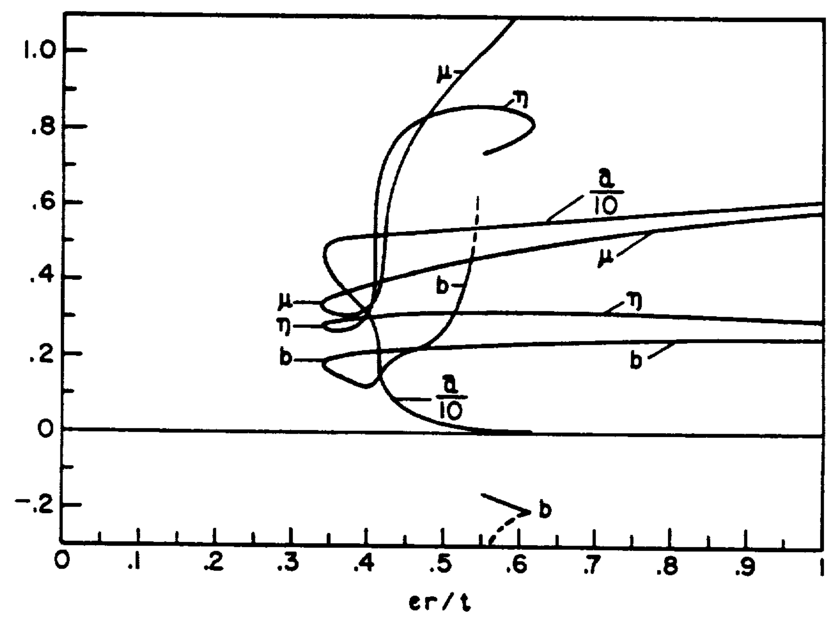

Figure 4.- Variation of deflection parameters with unit end shortening. Case IV: $A = .5$; $\eta_o = .1$; $\mu_o = .2$; $V = .01$.

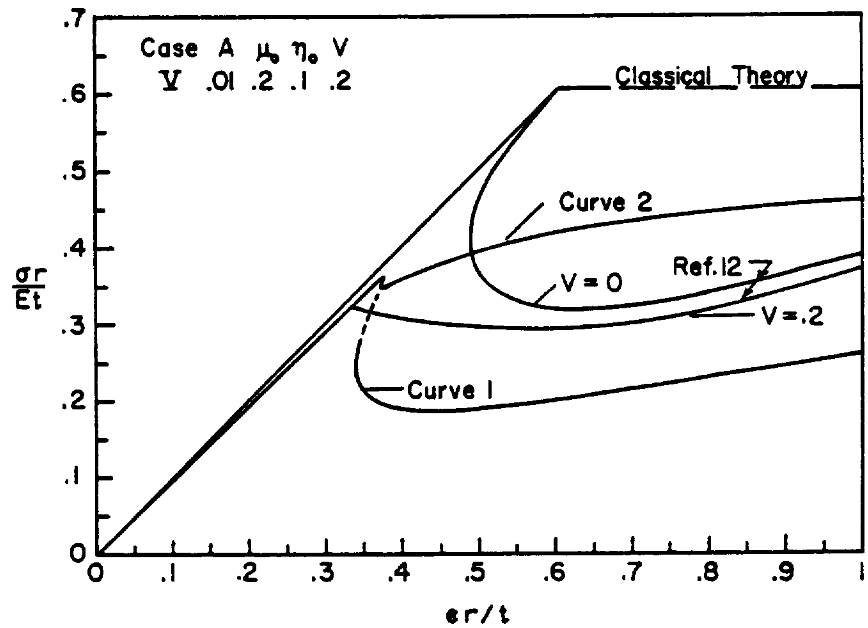

Figure 5.- Variation of applied stress with unit end shortening.

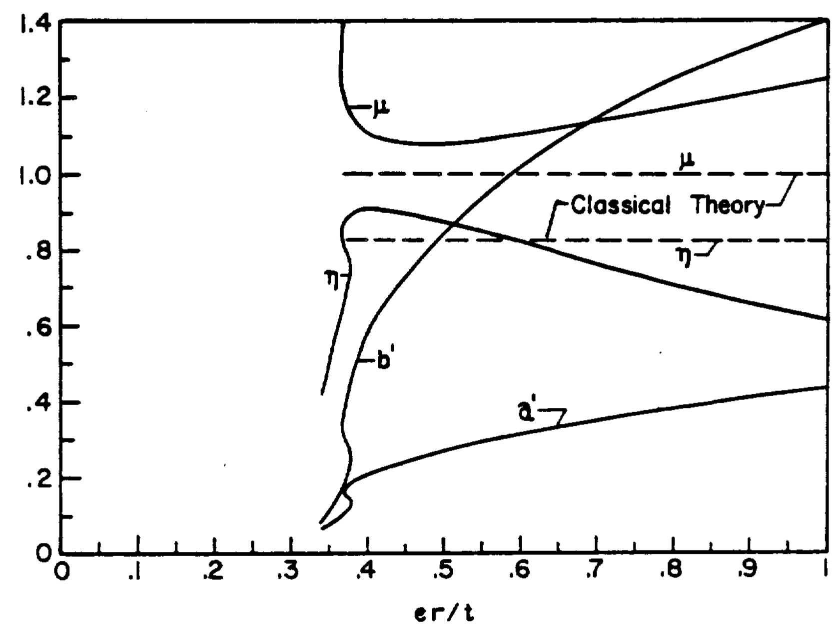

Figure 6.- Variation of deflection parameters with unit end shortening.
Case V: $A = .01$; $\eta_o = .1$; $\mu_o = .2$; $V = .2$.